

Development of wind vortex shedding coefficients for a multisided cylinder structure

Byungik Chang^{*1}, Michael Neill^{2a}, Roy Issa^{3b} and Aaron Miller^{3c}

¹University of New Haven, West Haven, Connecticut 06516, USA

²Phillips 66 Borger Refinery, Borger, Texas 79007, USA

³West Texas A&M University, Canyon, Texas 79015, USA

(Received October 19, 2012, Revised October 27, 2013, Accepted October 29, 2013)

Abstract. A major problem with high-mast light poles is the effects that wind vortex shedding can have on the pole itself because of the lock-in phenomenon. It is desired that the coefficients in the AASHTO Standard Specifications (5th edition) for Structural Supports for Highway Signs, Luminaries, and Traffic Signals be analyzed and refined. This is for the belief that the span of the shapes of poles for which the coefficients are used is much too broad and a specific coefficient for each different shape is desired. The primary objective of this study is to develop wind vortex shedding coefficient for a multisided shape. To do that, an octagonal shape was used as the main focus since octagonal cross sectioned high-mast light poles are one of the most common shapes in service. For the needed data, many wind parameters, such as the static drag coefficient, the slope of aerodynamic lift coefficient, Strouhal number, the lock-in range of wind velocities producing vibrations, and variation of amplitude of vortex-induced vibration with Scruton number are needed. From wind tunnel experiments, aerodynamic parameters were obtained for an octagonal shape structure. Even though aerodynamic coefficients are known from past test results, they need to be refined by conducting further wind tunnel tests.

Keywords: high mast light pole; fatigue design; vortex shedding; slender support structures; wind tunnel testing; simulation

1. Introduction

Cantilevered signal, sign, and light support structures are used nationwide on major interstates, national highways, local highways, and at local intersections for traffic control purposes. There have been a number of failures of these structures that can likely be attributed to fatigue. In Iowa (Dexter 2004), a high-mast light pole (HMLP), which is typically used at major interstate junctions, erected for service in 2001 along I-29 near Sioux City collapsed in 2003 (see Fig. 1 (a)). Fortunately, the light pole fell onto an open area parallel to the interstate and injured no one. Fig. 1 (b) shows another high-mast lighting tower failure in Colorado (Rios 2007) that occurred in 2007.

*Corresponding author, Associate Professor, E-mail: bchang@newhaven.edu

^a Maintenance Engineer, E-mail: keegan.neill@p66.com

^b Associate Professor, E-mail: rissa@wtamu.edu

^c Research Assistant, E-mail: ajmiller1111@gmail.com



Fig. 1 A collapsed high-mast light pole

Similar to the failure in South Dakota, the fracture initiated at the weld toe in the base plate to pole wall connection, and then propagated around the pole wall until the structure collapsed. It appears that these structures may have been designed based on incomplete or insufficient code provisions which bring reason to reevaluate the current codes that are in place.

There would be more causes of structure failure for slender support structures. Pre-existing cracks at base connection, galvanization-induced cracks, and extreme temperature change could reduce the fatigue resistance of a structure. Ultrasonic inspection has indicated the presence of weld toe cracks at the shaft-to-base-plate connections of some galvanized HMLP in Texas. These galvanization-induced cracks significantly decrease the fatigue life of welded details. However, the specific factors that could cause galvanization-induced fatigue cracking are not well understood (Dawood 2013). Extremely large loads such as high winds could cause brittle fractures while cyclic vibration such as diurnal variation of temperature in the metallic material could affect the structures during their lifetime (Constantinescu 2013).

A luminary support structure or HMLP is generally susceptible to two primary types of wind loading induced by natural wind gusts, or buffeting and vortex shedding, both of which excite the structure dynamically and can cause fatigue damage (AASHTO 2009). Vortex shedding is a unique type of wind load that alternatively creates areas of negative pressures on either side of a structure normal to the wind direction. This causes the structure to oscillate transverse to the wind direction. When the vortex shedding frequency (i.e., the frequency of the negative pressure on one side of the structure) approaches the natural frequency of the structure, there is a tendency for the vortex shedding frequency to couple with the frequency of the structure (also referred to as “lock-in” phenomenon) causing greatly amplified displacements and stresses.

While vortex shedding occurs at specific frequencies and causes amplified vibration near the natural frequencies of the structure, buffeting is a relatively “broad-band” excitation and includes frequencies of eddies that are present in the natural wind as well as those caused by wind-structure interactions. The dynamic excitation from buffeting can be significant if the mean wind speed is high, the natural frequencies of the structure are below 1 Hz, the wind turbulence intensity is high with a wind turbulence that is highly correlated in space, the structural shape is aerodynamically odd with a relatively rough surface, and the mechanical damping is low. In practice, a structure is always subject to both vortex shedding and buffeting excitations. But unlike vortex shedding,

where amplified dynamic excitation occurs within a short range of wind speeds, buffeting loads keep increasing with higher wind speeds.

Numerous studies have been completed to look at various aspects of wind induced vibration and the modeling of support structures. A current AASHTO design specification was developed based on NCHRP reports 469 (Dexter 2002) and 494 (Fouad 2003), which provides a comprehensive assessment of the design provisions developed in NCHRP Reports 411 (Fouad 1998) and 412 (Kaczinski 1998). According to NCHRP Report 469 and the long-term monitoring of HMLPs in Iowa (Chang 2009), some of slender support structures observed vortex shedding vibration in higher modes and damping ratio in higher modes are less than the recommended damping ratio of 0.5%. A newer version of design specification is being prepared based on NCHRP Report 718 (Connor 2012) which fatigue loading provisions for high-mast lighting towers are differentiated from those associated with other traffic structures. The Ontario Highway Bridge Design Code (2006) contains provisions for the design of support structures for vortex shedding. The provisions require that a structure be designed based upon the results of a dynamic modal analysis to solve for the amplitude of the steady-state response due to an applied force per unit length in the transverse direction. In addition, the Ontario specification recommends that vortex shedding pressures be applied over the length of a tapered member for which the cross-sectional member dimension is within 10% of the critical dimension and a vortex shedding coefficient (C_s) is used for design in the specification.

The use of wind tunnels to aid in structural design and planning has been steadily increasing in recent years (Liu 1991). Kitagawa (1997) conducted a wind tunnel experiment using a circular cylinder tower to study the characteristics of the across-wind response at a high wind speed. The authors found from the tests that both the vortex induced vibration at a high wind speed and the ordinary vortex induced vibration were observed under uniform flow.

Bosch and Guterres (2001) conducted wind tunnel experiments to establish the effects of wind on tapered cylinders using a total of 53 models representing a range of cross sections, taper ratios, and shapes (circular, octagonal, or hexagonal cross section), which were intended to be representative of those commonly found in highway structures. In a test of drag coefficient versus Reynolds number for the uniform circular cylinders, the results showed a consistent trend of convergence with a range of Reynolds numbers for which the drag coefficient flattens out to a constant value. It was also found that the introduction of a taper ratio significantly altered the aerodynamic behavior of the cylinder shapes (Chang 2009, 2010).

Garrett (2003) studied flow-induced vibration of elastically supported rectangular cylinders for his doctoral research. Wind tunnel experiments by James (1976) were performed to establish the effects of wind on uniform cylinders using several models representing a range of shapes (octagonal, dodecagonal and hexdecagonal cross section), model orientations, and corner radii based on Reynolds number (R_e) between 2.0×10^5 and 2.0×10^6 . Lift and drag coefficients were developed for an octagonal cylinder by Simui and Scanlan (Blevins 1990). In the study, the slope of the mean drag coefficient (C_D) was found to be near zero and the slopes of the mean lift coefficient (C_L) were calculated to be approximately $-1.7 \cdot \pi$ for flat orientation and $0.45 \cdot \pi$ for corner orientation.

Recent research efforts related to the subject matter of this study have used commercial computer simulation along with physical measurement devices to explore vortex induced vibration (VIV) and vortex shedding of circular and polygonal cylindrical shapes and other slender structures. Circular cylinders and octagonal cylinder have similar wake features and aerodynamics coefficients. Cylinder displacement and VIV in cross-flow have been proven to be predicted

accurately by commercial code in recent years (Placzek 2009). The results matched with experiments and other, similar numerical studies. However, these results only were tested at low Reynolds numbers and without structural dampening. A recent study also has investigated VIV with observation equipment. A traffic-signal-support with cantilevered mast arms was studied because it was known to exhibit large-amplitude vibrations under some wind conditions (Zuo 2010). A full-scale, installed support structure was measured to determine the role of the cantilevered mast arm in aeroelastic vibrations. The study revealed that the mast arm was a critical mechanism in the vibrations. The VIV's were found to cause the largest amplitude vibrations at low wind speeds. A finite element model (FEM) based study developed the natural frequency equations for long tapered hollow poles as functions of their geometric variables (Le 2008). The model accounted for couplings between material, contact, and geometric nonlinearities. The FEM results were verified with experimental data obtained from monitoring a 60 ft light pole. A sensitivity study also was conducted to identify the effect of different geometric parameters on the natural frequencies of the pole. Using the equations generated by this method, a mechanical damping device can be developed to dissipate wind-induced vibrations based on the geometric properties of the pole.

The primary objective of this study was to develop wind vortex shedding coefficient for an octagonal shape. In this study, an octagonal shape was the main focus since octagonal cross sectioned high mast light poles are one of the most common shapes in most states. To be able to calculate the needed data for the structure, many wind parameters, such as the static drag coefficient, the slope of aerodynamic lift coefficient, Strouhal number, the lock-in range of wind velocities producing vibrations, and variation of amplitude of vortex-induced vibration with Scruton number, are needed. From wind tunnel experiments, aerodynamic parameters were obtained for an octagonal shape structure. Even though aerodynamic coefficients are known from past test results, they need to be refined by conducting further wind tunnel tests.

2. Wind tunnel testing

Wind tunnel testing is widely used in many applications to study the different aerodynamic flows and effects on certain types of structures and components, whether the test specimens are typically or unusually shaped. To be able to determine the wind induced loads on a structure there are certain aerodynamic parameters that must be obtained to do so. These parameters consist of a few, but not limited to, the Strouhal number, drag and lift coefficients, Scruton number, etc. The problem is that only few references are available to provide values for some of these parameters, and only in a certain range of Reynolds numbers for the octagonal shape that is undergoing the study. Therefore, it is necessary to do several wind tunnel tests to ultimately determine the wind vortex shedding coefficients of the octagonal structure being tested.

2.1 Wind tunnel

The wind tunnel that is used for this case is the Bill James Open Circuit Wind Tunnel (see Fig. 2), which is located in the Wind Simulation and Testing Laboratory (WiST Lab) at Iowa State University, Ames. This is a suction orientation wind tunnel with a 22:1 contraction ratio. The wind tunnel test section is of the dimensions 3 ft \times 2.5 ft (91.4 cm \times 76.2 cm) and 8 ft (2.44 m) length

following the contraction exit. The test section has an acrylic viewing window next to the wind tunnel control/data station with an access door opposite the side of the station. The fan, which is located downstream of the test section, is powered by a 100hp, 3-phase, 440 volt motor. The fan is controlled either by an analog remote control knob which is located at the wind tunnel control station and connected to the variable frequency fan, or directly by using the digital control screen mounted on the actual motor control power box. The fan speed can be changed in minimal steps of 0.1 Hz or approximately 0.51 ft/s (0.16 m/s) using these controls.

2.2 Test model

For all of the tests, a wooden cylindrical model with an octagonal (8-sided) cross section of diameter 4 in. (10.2 cm, face to face distance) and length of 20 in. (50.8 cm) was used. These dimensions were selected based on the need to maintain a wind tunnel blockage criterion of 8% or less. The actual blockage was 7.4% and, therefore, blockage effects could be neglected. The length of the model, 20 inches (50.8 cm), was chosen to maximize the area of the model that would be exposed to the air stream while at the same time leaving enough room on both sides of the model to attach any additional fixtures that are required in order to change certain parameters. Fig. 3(a) shows a schematic diagram of the test model.

End plates, which are made out of clear plastic, were attached to the model to minimize the three-dimensional end effects on the model and to, in turn, maintain a two-dimensional flow on the model. To test multiple modifications of the model with a different mass, pairs of commercially available C clamps were clamped to the end plates at equal distances from the centerline of the model to avoid any torsion.

2.3 Dynamic test

Many tests were conducted on the model to obtain all of the many needed aerodynamic parameters. Results of most importance include Strouhal number, lock-in range of wind velocities for vortex shedding, and the amplitude of vortex-induced vibrations as a function of the Scruton number.

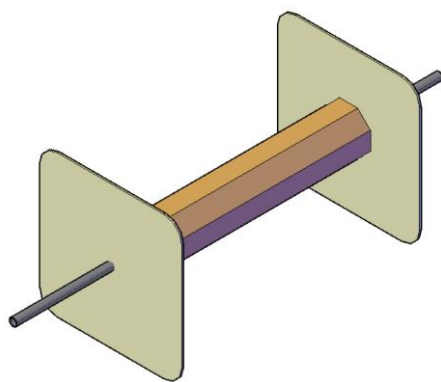
For the dynamic test, the vertical motion dynamic setup was designed to allow only a single-degree-of-freedom, which means that the test model was designed to only allow motion along the vertical axis perpendicular to the wind direction. The model was suspended by a set of eight linear coil springs and chains, with four of each on each side of the model. Two cantilever type force transducers were used with one placed at the top and one at the bottom, at diagonally opposite springs.

2.4 Spring suspension system

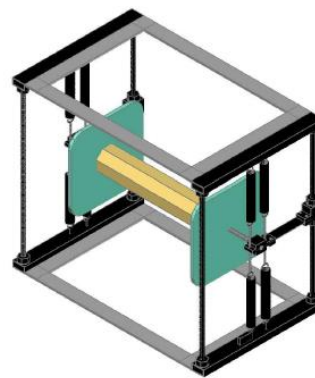
The spring suspension system was attached to a frame that was fixed to the test section floor and ceiling immediately adjacent to the side walls. A load cell frame was constructed with small structural channels and the 0.625 in. (15.875 mm) diameter aluminum alloy rod was installed by sliding the rod through a 0.75 inch (19.05 mm) diameter hole at the center of the block and the center of the wooden model a collar was then slid over each end of the rod and attached to the block that helped to clamp the model to the rod with a set of screw. Fig. 3(b) is a schematic diagram of the dynamic test suspension system.



Fig. 2 Bill James Wind Tunnel at Iowa State University



(a) octagonal test model



(b) dynamic suspension system

Fig. 3 Schematic diagrams

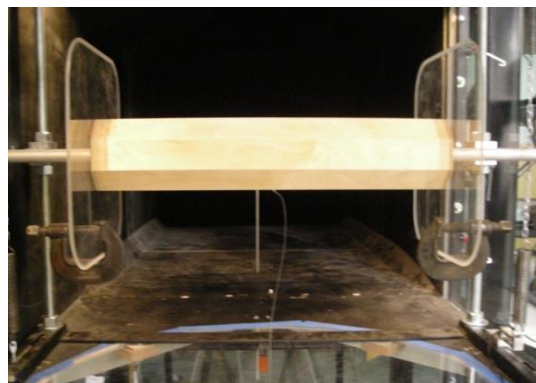


Fig. 4 Configuration of test orientation

2.5 Experimental procedure

As can be seen in Fig. 4, the section model with the flat orientation and end plates was suspended from the frame by eight linear coil springs. The model was tested over a range of wind speeds that end up producing vortex induced vibrations. The wind speeds were increased at the least by 0.1 Hz of fan speed with the AC motor controller, with the initial fan speed at 0.5 Hz. Each increment of fan speed corresponds with approximately 0.51 ft/s (0.16 m/s) of wind speed with 0.5 Hz being equal to 3.5 ft/s (1.07 m/s). The dynamic test procedures were established in order to obtain the Strouhal number, the range of wind velocities producing vortex induced vibrations, and the variation of amplitude of vortex induced vibration with the Scruton number.

3. Test results

From the previously described wind tunnel tests, it was possible to obtain several aerodynamic parameters such as the static drag coefficient, the slope of the aerodynamic lift coefficient, the Strouhal number, the lock-in range of wind velocities, and the amplitude of vortex induced vibration as a function of the Scruton number.

A dynamic suspension system was designed to allow only single-degree-of-freedom vibration of the model along the vertical axis. The model was suspended by eight linear coil springs, and chains, four on each side. The natural frequency, stiffness, damping, and mass of the system will be described in this section. The test was conducted for flat orientation, as shown in Fig. 4. The following results will be described for both the flat and corner orientation.

3.1 Lock-in range and Strouhal number

The model, as said before, was tested over a wide range of wind speeds that would produce vortex induced vibrations. Fig. 5 shows the response of the model in the lock-in region of a freely vibrating cylinder. As can be seen in the figure, the highest amplitudes were achieved in a distinct range of the reduced velocity.

The lock-in range and Strouhal number ($f_s \cdot D/U \approx 0.17$) are shown in Fig. 6. Lock-in occurs when the vortex shedding frequency matches the natural frequency of the actual system which occurs at a critical wind speed causing the response at the lock-in region to be much larger than that of the normal region. The lock-in region stays consistent over a certain range of wind speeds as shown in Fig. 6, which shows that the lock-in region was in a range of reduced velocities from 5.5 to 6.5.

Fig. 7 shows the frequency spectrum of the displacement response of the elastically supported cylinder for the three different instances of (a) before lock-in, (b) at lock-in, and (c) after lock-in, all for the flat orientation, where f_s and f_n are the vortex-shedding frequency and the natural frequency, respectively, of the test model. These figures show that the model produces much higher amplified displacements when the vortex shedding frequency and the natural frequency match one another.

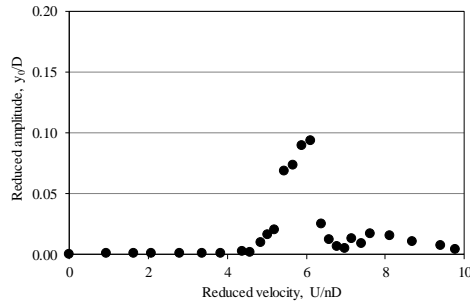


Fig. 5 Vortex-induced vibration of an octagonal shape cylinder

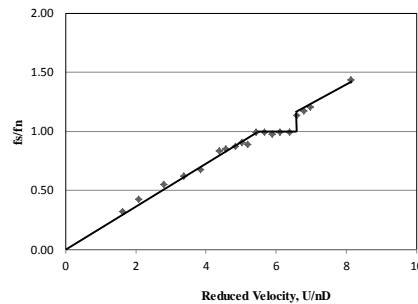


Fig. 6 Lock-in range for an octagonal shape cylinder and Strouhal number

3.2 Scruton number

The amplitude of the model is directly related to the Scruton number (S_c). In order to determine the amplitude versus the Scruton number, it was necessary to obtain several different parameters. These parameters include the inertial mass, stiffness, natural frequency, and the system damping ratio. The Scruton number is solved using Eq. (1).

$$S_c = \frac{m \cdot \zeta}{\rho \cdot D^2} \quad (1)$$

where, m is mass per unit length, ζ is a damping ratio, ρ is air density, and D is the cross-wind dimension of the cross-section.

The inertial mass, stiffness, and natural frequency for each case were determined using the added mass method, by adding masses incrementally. This was done by testing multiple specimens of the model with different masses, added by clamping pairs of commercially available C-clamps with different weights to the previously described plastic end plates. A total of five pairs of clamps and one thin steel plate were used. To avoid the introduction of torsion on the testing model, the clamps and the steel plate were added to the plastic end plates on opposite sides of the cylinder. The system damping was determined for each case experimentally by using the logarithmic decrement method.

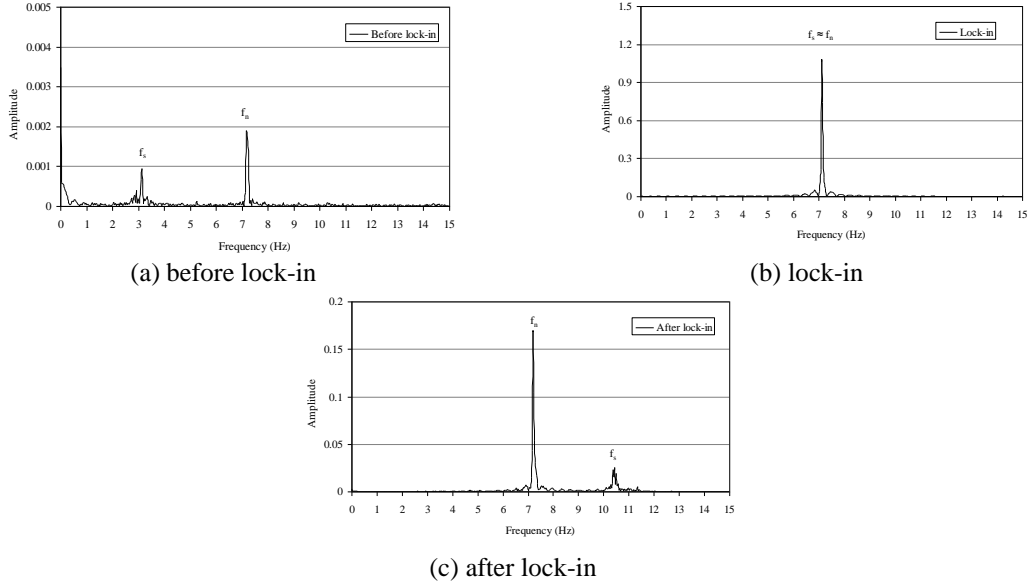


Fig. 7 Frequency spectra of displacement response of cylinder

The system natural frequency can be expressed as

$$\omega_n = \sqrt{\frac{k}{m}} \quad \text{or} \quad \omega_n^2 = \frac{k}{m} \quad \text{or} \quad \frac{1}{\omega_n^2} = \frac{m}{k} \quad (2)$$

where, ω_n is the natural frequency of the system and k and m are the stiffness and mass, respectively.

The above equation can be expressed in terms of the added mass (M_{add})

$$\frac{1}{\omega_i^2} = \frac{m + M_{add}}{k} \quad (3)$$

Table 1 summarizes the added mass and corresponding natural frequency and damping ratio. A plot for the added mass versus the inverse of the square of the circular frequency is shown in Fig. 8 along with a best-fit line. The figure shows that the inverse of the square of the circular frequency is linearly proportional to the added mass. The intercept of the y-axis ($1/\omega_n^2$, at added mass of zero) and the slope of the best fit line was determined to be 0.00053704 and 0.00271255, respectively. The square root of the inverse of the intercept value was determined to be 43.15 rad/sec. It was also possible to determine the stiffness of the system, which was calculated by taking the inverse of the slope, coming out to be 368.66 lb/ft. The inertial mass of the system, without added mass, can be determined by using Eq. (3), as 0.198 slugs. Table 2 lists the system frequency, stiffness, and inertial mass that were calculated using the best fit line. The Scruton number (S_c) for each case of added mass was calculated using Eq. (1) and the reduced amplitude (y_o/D , max amp./diameter of the model) was obtained from the measurement that was taken when the maximum displacement occurred. The best fit line was also plotted and is shown in Fig. 9.

Table 1 System frequencies with added mass (1 lb/ft = 14.6 N/m and 1 slug = 14.6 kg)

Weight kg	Added Weight		Weight lb	Mass slugs	Freq. Hz	Period	Freq. rad/s	$1/\omega^2$ s^2/rad^2	Damping %	Adj.mass slugs
2.046	0.00	0.00	4.51	0.00	6.879	0.145	43.22	0.000535	0.1082	0.197
2.717	0.67	1.51	5.99	0.05	6.205	0.161	38.99	0.000658	0.1648	0.243
3.675	1.63	3.66	8.10	0.11	5.469	0.183	34.36	0.000847	0.1927	0.310
4.613	2.57	5.77	10.17	0.18	4.950	0.202	31.10	0.001034	0.1766	0.376
5.421	3.38	7.58	11.95	0.24	4.670	0.214	29.34	0.001161	0.1721	0.432
6.270	4.22	9.49	13.82	0.29	4.335	0.231	27.24	0.001348	0.1620	0.491
7.139	5.09	11.44	15.74	0.36	4.109	0.243	25.82	0.001500	0.2028	0.552
9.027	6.98	15.68	19.90	0.49	3.700	0.270	23.25	0.001850	0.2139	0.683
10.353	8.31	18.66	22.82	0.58	3.457	0.289	21.72	0.002120	0.2390	0.776
11.989	9.94	22.33	26.43	0.69	3.240	0.309	20.36	0.002413	0.1861	0.890

Table 2 Adjusted system frequency and mass (1 lb/ft = 14.6 N/m and 1 slug = 14.6 kg)

Frequency rad/s	Frequency Hz	Stiffness lb/ft	Adjusted Mass Slugs	Weight lb
43.15	6.87	368.7	0.198	3.375

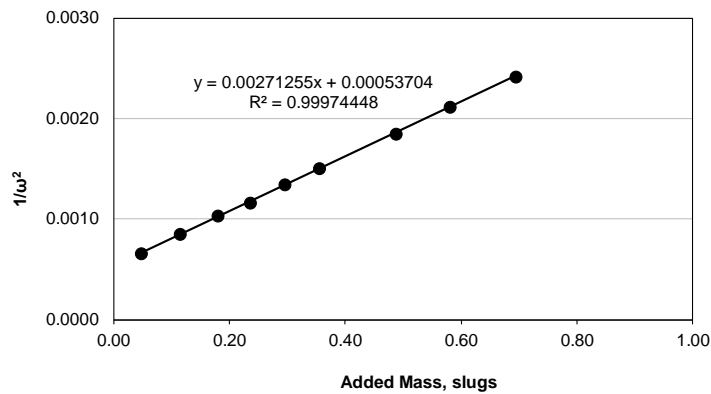


Fig. 8 Inertial mass identification of cylinder (1 slug = 14.6 kg)

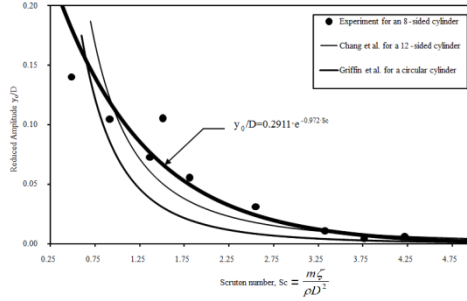


Fig. 9 Scruton number vs. maximum amplitude for the octagonal cylinder

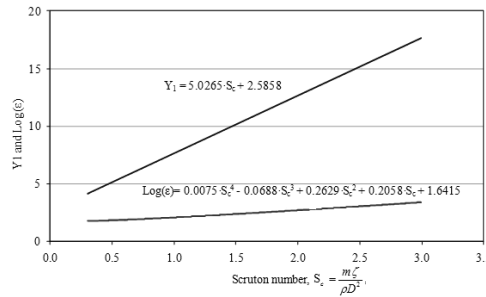


Fig. 10 Aerodynamic damping parameters during “lock-in”

4. Mathematical model for vortex shedding induced response

Since vortex shedding is for the most part a sinusoidal process, it is reasonable to model the vortex shedding transverse force imposed on a circular cylinder as harmonic in time at the shedding frequency (Simiu 1996). The time varying force, $F_{vy}(t)$, in Scanlan’s model, can be expressed as

$$F_{vy}(t) = \frac{1}{2} \cdot \rho \cdot U^2 \cdot A \cdot \left[Y_1(k) \cdot \left(1 - \varepsilon \cdot \frac{y^2}{D^2}\right) \cdot \frac{\dot{y}}{U} + Y_2(k) \cdot \frac{y}{D} + \tilde{C}_L(k) \cdot \sin(\omega_n \cdot t + \phi) \right] \quad (4)$$

where U is the wind velocity, A is projected area of the structure, Y_1 , ε , & Y_2 are aerodynamic functions of reduced frequency k , at lock-in, D is the cross-wind dimension of the cross-section, \tilde{C}_L is the rms of lift coefficient, ω_n is the natural frequency, t is time, and ϕ is the phase angle.

The aerodynamic damping parameters, Y_1 and ε are functions of the Scruton number (S_c) as shown in Fig. 10 at “lock-in”. Fig. 10 is a graphical representation extracted from Eq. (5) (Simiu 1996) from wind tunnel tests of steady-state amplitudes y_0 of different test cases corresponding to different S_c during “lock-in”. Y_1 and ε are constant during the lock-in but they are different at different S_c . Thus, Y_1 and ε are generated using any of two measurements for y_0/D and the averaged S_c . It was assumed that Y_1 and ε are zero outside the lock-in range and Y_2 and are not considered here since these have insignificant effects on the response for the analysis of Eq. (4).

$$\frac{y_0}{D} = 2 \left[\frac{Y_1 - 8\pi \cdot S_c \cdot S_t}{\varepsilon \cdot Y_1} \right]^{1/2} \quad (5)$$

where, y_0/D is the reduced amplitude, S_c is the Scruton number, S_t is the Strouhal number.

5. Conclusions

There have recently been many failures of High Mast Light Poles (HMLP). For this reason, there was a need to dive deeper into the process of the design that is being used for these structures. It is broadly accepted that there is considerable uncertainty in the calculation of wind induced loads in the AASHTO Standard Specifications (2009) for Structural Supports for Highway Signs, Luminaries, and Traffic Signals. The main uncertainty in this case being that the certain coefficients being used, such as the Strouhal number, are too conservative.

The primary objective of this study was to develop a wind vortex shedding coefficient for an octagonal shape. This would help fatigue design for slender support structures. In order to develop the fatigue design procedure for wind-induced pressures on a structure, several wind parameters, such as the static drag coefficient, the slope of aerodynamic lift coefficient, Strouhal number, the lock-in range of wind velocities producing vibrations, and variation of amplitude of vortex-induced vibration with Scruton number, are required. Based on wind tunnel experiments, aerodynamic parameters were obtained for an octagonal shape structure. Although several aerodynamic coefficients are known from past wind-tunnel test results, they needed to be refined based on further wind tunnel tests. The following conclusions can be drawn based on the current study:

- The Strouhal number (S_t) for an octagonal shape was determined to be approximately 0.17. As a reference, the Strouhal number for a circular shape is 0.2 and Chang et al. found it to be 0.2 for a 12-sided cylinder. Additionally, the current AASHTO standard specification uses 0.15 for multi-sided cross sections for design purposes and this seems to be reasonable for a conservative design after the findings of this research project and others.
- The Scruton number vs. maximum amplitude for the octagonal cylinder shows a similar trend curve but higher amplitude than the circular shape while it is fairly close to the 12-sided cylinder curve. The equation in this case for the octagonal shape was not feasible enough to be used in the same format as was Griffin's or Chang's for a 12 sided cylinder. Instead, an equation in the format of exponential decay was derived.
- The aerodynamic damping parameters, Y_l and ε are functions of the Scruton number during "lock-in". These were extracted from the wind tunnel experimental observations of steady-state amplitudes of the model at "lock-in". Y_l looks to have a linear relationship with respect to the Scruton number while ε shows a nonlinear relationship.

The following recommendations can be drawn based on the current study:

- A simplified Scanlan's Van-der Pole Oscillator model with the aerodynamic damping coefficients (Y_l and ε) would improve the vortex shedding-induced load for fatigue design of highway support structures.
- Higher natural frequencies should be strongly recommended for the critical wind velocity

at which vortex shedding lock-in occurs.

- A more conservative damping ratio should be considered depending on the natural frequency of a structure, especially in higher modes. The current recommended damping ratio is 0.5% and NCHRP Report 469 and other study show vortex shedding vibration can occur in higher modes.

Acknowledgements

The authors thank Iowa State University WiST laboratory and Dr. Partha Sarkar for allowing the use of the Wind Tunnel and data acquisition system for the testing and collection of data for the project.

References

- American Association of State Highway and Transportation Officials. (2009), *Standard specifications for structural support for highway signs, Luminaries, and Traffic Signals*, 5th Ed., Washington, D.C.
- Belver, A.V., Ibán, A.L. and Lavín Martín, C.E. (2012), “Coupling between structural and fluid dynamic problems applied to vortex shedding in a 90m steel chimney”, *J. Wind Eng. Ind. Aerod.*, **100**(1), 30-37.
- Blevins, R.D. (1990), *Flow-induced vibration*, 2nd Ed., Van Nostrand Reinhold, New York.
- Bosch, H.R. and Guterres, R.M. (2001), “Wind tunnel experimental investigation on tapered cylinders for highway support structures”, *J. Wind Eng. Ind. Aerod.*, **89**(14), 1311-1323.
- CAN/CSA-S6-06 (2006), *Canadian highway bridge design code*, CAN/CSA-S6-06, CSA International, Rexdale, Ontario, Canada.
- Chang, B.e.a. (2009), “Development of a procedure for fatigue design of slender support structures subjected to wind-induced vibration”, *J. Trans. Res. Board*, **2131**, 23-33.
- Chang, B.e.a. (2010), “Time-domain model for predicting aerodynamic loads on a slender support structure for fatigue design”, *J. Eng. Mech. - ASCE* **136**(6), 736-746.
- Connor, R.J., Collicott, S.H., DeSchepper, A.M., Sherman, R.J. and Ocampo, J.A. (2012), NCHRP Report 718: *Fatigue Loading and Design Methodology for High-Mast Lighting Towers*. TRB, National Research Council, Washington D.C.
- Constantinescu, G.e.a. (2013), *Wind loads on dynamic message cabinets and behavior of supporting trusses*. Final report to Iowa Department of Transportation, Ames, Iowa.
- Dawood, M., Goyal, R., Dhonde, H. and Bradberry, T. (2013), “Fatigue life assessment of cracked high mast illumination poles”, *J. Perform. Constr. Fac.*, In press.
- Dexter, R.J. and Ricker, M.J. (2002), NCHRP Report 469: *Fatigue-resistant design of cantilever signal, sign, and light supports*. TRB, National Research Council, Washington D.C.
- Dexter, R.J. (2004), *Investigation of cracking of high-mast lighting towers*. Final report to Iowa Department of Transportation, Ames, Iowa.
- Fouad, F.H., Calvert, E.A. and Nunez, E. (1998), NCHRP Report 411: *Structural supports for highway signs, luminaries, and traffic signals*, TRB, National Research Council, Washington, D.C.
- Fouad, F.H., Calvert, E.A. and Nunez, E. (2003), NCHRP Report 494: *Structural supports for highway signs, luminaries, and traffic signals*, TRB, National Research Council, Washington, D.C.
- Garrett, J.L. (2003), *Flow-induced vibration of elastically supported rectangular cylinders*, Ph.D. dissertation, Iowa State University, Ames, Iowa.
- James, W.D. (1976), *Effects of Reynolds number and corner radius on two-dimensional flow around octagonal, dodecagonal and hexdecagonal cylinders*, Ph.D. dissertation, Iowa State University.
- Kaczinski, M.R., Dexter, R.J. and Van Dien, J.P. (1998), NCHRP Report 412: *Fatigue resistance design of*

- cantilevered signal, sign, and light supports*, TRB, National Research Council, Washington, D.C.
- Kitagawa, T., Wakaharab, T., Fujinob, Y. and Kimurab, K. (1997), "An experimental study on vortex-induced vibration of a circular cylinder tower at a high wind speed", *J. Wind Eng. Ind. Aerod.*, **69-71**, 731-744.
- Le, T., Abolmaali, A., Ardavan Motahari, S., Yeih, W. and Fernandez, R. (2008), "Finite element-based analyses of natural frequencies of long tapered hollow steel poles", *J. Constr. Steel Res.*, **64**(3), 275-284.
- Liu, H. (1991), *Wind engineering*, Prentice Hall, New Jersey.
- Placzek, A., Sigrist, J.F. and Hamdouni, A. (2009), "Numerical simulation of an oscillating cylinder in a cross-flow at low Reynolds number: Forced and free oscillations", *Comput. Fluids.*, **38**(1), 80-100.
- Rios, C. (2007), *Fatigue performance of multi-sided high-mast lighting towers*, MS Thesis, The University of Texas at Austin, Austin, Texas.
- Simiu, E. and Scanlan, R.H. (1996), *Wind effects on structures, fundamentals and applications to design*, 3rd Ed., John Wiley & Sons, New York, NY.
- Zuo, D. and Letchford, C.W. (2010), "Wind-induced vibration of a traffic-signal-support structure with cantilevered tapered circular mast arm", *Eng. Struct.*, **32**(10), 3171-3179.